JOURNAL OF APPLIED ELECTROCHEMISTRY 8 (1978) 281–285

# The rotating electrolyser. I. The velocity field

R. E. W. JANSSON, R. J. MARSHALL, J. E. RIZZO

*Chemistry Department, Southampton University, Southampton, UK*

Received 18 July 1977

A rotating electrolyser is described briefly in which, in principle, anolyte and catholyte streams can be segregated without a diaphragm. Laser–Doppler anemometry has been used to measure the velocity field in such an electrolyser and has shown that, despite the flow field being more complex than described by first order theory, the concept is valid.

## Symbols

| | |
|---|---|
| $a$ | semi-gap |
| $Q$ | volumetric flow rate |
| $\bar{r}$ | radius |
| $r = \alpha\bar{r}/a$ | dimensionless radius |
| $(Re) = Q/4\pi a\nu$ | Reynolds number |
| $\bar{u}$ | radial velocity |
| $u = \bar{u}4\pi a^2/Q$ | dimensionless radial velocity |
| $v$ | tangential velocity |
| $z = \alpha\bar{z}/a$ | non-dimensional distance |
| $\bar{z}$ | measured distance from axial plane |
| *Subscripts* | |
| i | inner |
| m | maximum |
| o | outer |
| *Greek* | |
| $\alpha = (a^2\omega/\nu)^{1/2}$ | Taylor number |
| $\nu$ | kinematic viscosity |
| $\omega$ | angular velocity |

## 1. Introduction

While many electrolyses may be performed successfully in an undivided cell, in general it is preferable to keep anolyte and catholyte streams apart. The most obvious way of doing this is with a diaphragm which, however, introduces an energy penalty and may in fact present other practical difficulties. There is also the common need to minimise the interelectrode gap to minimize resistive losses in the electrolyte, particularly in organic systems where conductivities are low. By operating under creeping-flow conditions [1] anode–cathode transport can be eliminated even at small gaps, and in fact many electrochemical reactors behave as if close to each electrode there is a slowly-moving phase with a faster-moving bulk phase between these anolyte and catholyte streams [2, 3] so that a diaphragm is not as necessary as is often supposed. However applications do arise where the streams must be separated while the presence of a diaphragm is undesirable. This can be achieved in a rotating electrolyser [4] in which source flow is established between two co-rotating discs.

Fig. 1 shows a schematic diagram of the rotating electrolyser in its simplest form [4]; it consists of two flat disc electrodes rotating together on a common shaft. Electrolyte is pumped radially outwards from the centre, or is induced to flow outwards if the electrolyser as a whole is immersed in a tank. In theoretical work relating to radial gas turbines Kreith [5] showed that, on rotation, the cubic–parabolic velocity profile of the radial outflow is progressively distorted as the Taylor number, $\alpha$, increases, the velocity near the wall growing at the expense of the velocity in the axial plane until the point at which $\alpha = \pi$ when the velocity in the midplane is zero (see also Fig. 2). This is a desirable condition for an electrolyser since, in effect, wall jets have been formed close to each electrode while most of the interelectrode fluid is near-stagnant. The anolyte and catholyte streams may then be permanently split at exit from the cell and stripped of product before being returned to the inlet for re-processing [4]; this system should be ideal for performing so-called 'paired' reactions [6].

The work reported here concerns the experimental investigation of the basic concept with a

 © 1978 *Chapman and Hall Ltd.* 

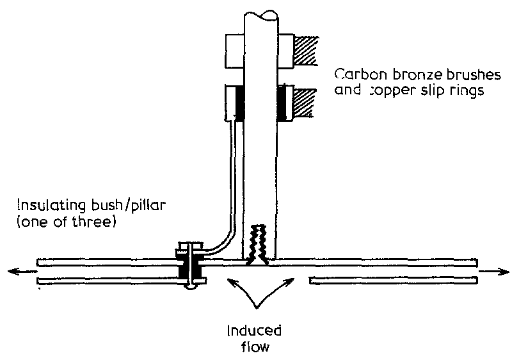


Fig. 1. Schematic diagram of rotating electrolyser (not to scale).

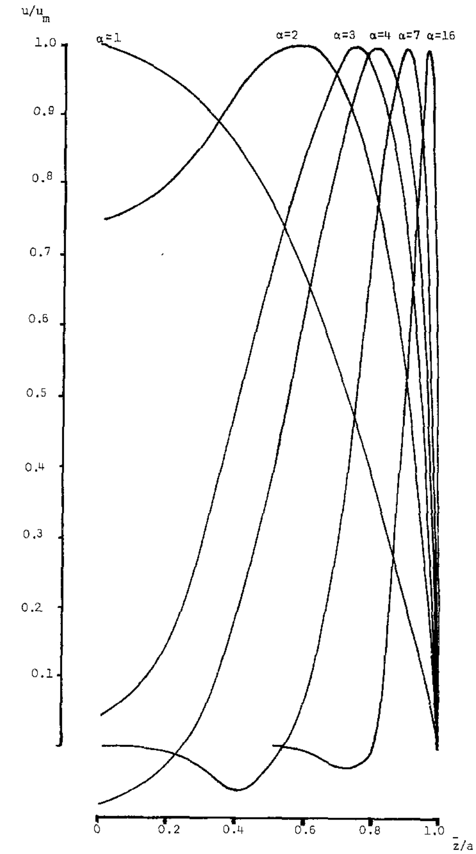


Fig. 2. Calculated normalized radial velocity profiles.

number of model cells; Part I deals with radial and tangential velocity distributions, while Part II is a description of mass transfer and related characteristics of the device.

## 2. Fluid Mechanics

The problem of rotating source flow has been treated theoretically by Kreith [5], who gives the non-dimensional radial velocity as

$$u = \frac{1}{r}\frac{4\alpha^2}{\sinh 2\alpha - \sin\alpha}\Big(\sinh\alpha\sin\alpha\cosh z\cos z - \cosh\alpha\cos\alpha\sinh z\sin z + \frac{\alpha^2(Re)}{r^2}F(z,\alpha) + \ldots\Big). \quad (1)$$

Note that the strength of the source, i.e. $Q \propto (Re)$, only appears in the second term along with $F(z, \alpha)$, which is a complicated term only obtained with difficulty [5]. Kreith evaluated the first term in Equation 1 for values of $\alpha$ up to $\pi$, exhibiting the formation of the double-humped radial velocity distribution. Fig. 2 shows the normalized velocity distribution calculated for values of $\alpha$ up to 16. As $\alpha$ increases the velocity maximum moves progressively towards the wall and forms a strong wall jet (Fig. 3); at $\alpha = 16$, for example, Equation 1 suggests that the jet occupies only 20% of the semi-gap, i.e. 10% of the interelectrode spacing. The electrochemical implications are obvious.

Since it is assumed that the fluid enters the device with no swirl, the tangential velocity profile is expected to be U-shaped, with a maximum on each wall and, possibly, some body rotation in between. With increasing radius the rotational motion of the fluid as a whole must increase but the tangential (wall) velocity also increases so the U-shape may be preserved and the velocity gradient at the wall may actually increase. The question then arises whether the interaction of radial and tangential motion will give rise to secondary flows which will so increase cross-gap mixing that the separation of streams implied by Equation 1 will be lost. To resolve this point and confirm the correctness of Kreith's theory, the velocity field was measured in a model electrolyser with laser Doppler anemometry. Tracer experiments were also performed which will be reported in Part II and elsewhere [7].

## 3. Experimental

Fig. 1 shows a schematic diagram of the cell; two flat nickel discs 176 mm in diameter and 2 mm thick were connected by three insulating pillars at 50 mm PCD where the tangential velocity was

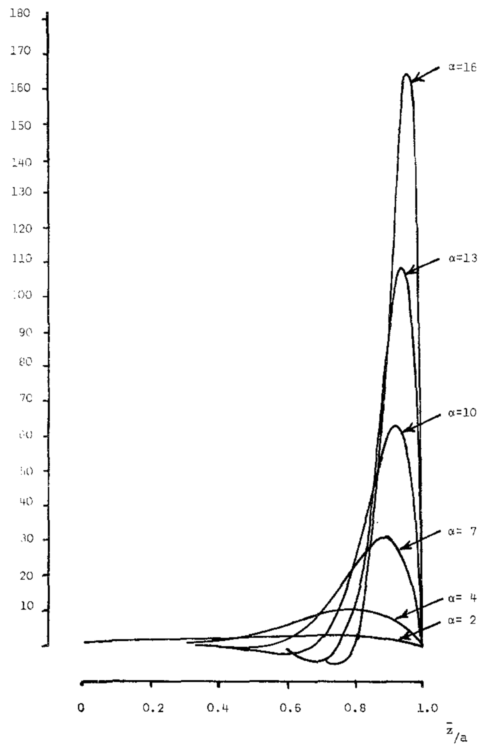


Fig. 3. Development of wall jet with Taylor number.

small and the disturbance to the flow least. The outer faces of the electrodes were coated in resistive paint. An entry hole 44 mm in diameter was cut in the lower disc, while the upper disc was connected to a shaft running vertically in ball bearings and driven by a slow-speed motor. The interelectrode gap could be adjusted by varying the height of the pillars (3·5 or 6·4 mm), which also acted as insulating bushes for the current connections to the lower plate. The shaft acted as a busbar for the upper plate. Carbon-bronze brushes and copper slip rings were used to make contact with the external circuit and an electronic tachometer fixed to the end of the shaft was used to count rotational speed. The plates were immersed in a square tank of electrolyte and rotation of the cell induced flow radially outwards between the plates, the square-sided tank being necessary to provide reasonably flat optical windows for the laser beams; free discharge would have made anemometry impossible. Since Equation 1 is insensitive to $Q$ it was hoped that the form of the velocity distribution would not be altered even though the cell was made to pump itself. A central feed from an external pump is the preferred method of operation for a practical electrolyser [4], but was thought to be an unnecessary complication at this stage.

A schematic diagram of the laser Doppler anemometer is shown in Fig. 4. The instrument has been developed to measure one or two components of the velocity vector in real time at any location in a field approximately 1 m × 100mm × 100 mm and is fully described elsewhere [8, 9]. Basically, light from a 20 mW He/Ne laser is passed through a partially opaque disc turning at low speed and part of the scattered light, defined by a mask (A), is focussed at the centre of interest (B) before being brought to the face of the photomultiplier by the lens system and pinhole (C). The beam transmitted through the disc is also focussed at the centre of interest and light scattered from it by the micron-sized particles in the flow is recombined with the disc-scattered beam on the face of the photomultiplier, giving rise to fluctuations in light intensity at a Doppler frequency which is the sum of the shift due to the particle velocity component in the plane of the beams and the shift due to the rotating disc. This allows

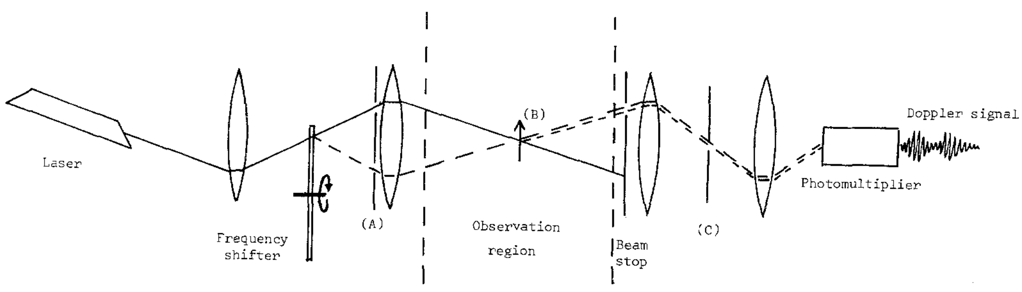


Fig. 4. Schematic diagram of laser–Doppler anemometer [8].

negative velocities (reversing flows) to be measured by applying a large positive bias with the turning disc. (There are no such things as negative frequencies, of course; a negative velocity gives rise to a positive frequency but with a phase shift that makes signal processing difficult). The Doppler frequency is tracked in real time by a frequency tracker which gives a voltage output proportional to frequency, hence velocity, so that instantaneous, mean and r.m.s. values of velocity can be obtained [8, 9]. Velocity fluctuations can also be autocorrelated or cross-correlated with other fluctuating quantities such as local current density [8, 10].

The laser anemometer was mounted as a whole on a stereotaxic table with three degrees of freedom, so that the radial and tangential velocity components could be measured at a number of radial and cross-gap stations by simply traversing the instrument with respect to the rotating electrolyser in its tank. Although the focal volume is only about 0·2 mm diameter, the greater beam width away from this point limited the distance of approach to an electrode to about 0·5 mm, at which distance the sudden deterioration in signal quality confirmed that the beam was grazing the surface. The same criterion was used to check flatness, coplanarity of the two discs and shimmy in the bearings, which totalled about ± 0·2 mm, which represents the maximum accuracy of location.

## 4. Results

Fig. 5 shows the normalized radial velocity distribution measured at a number of radial locations, $r/r_o$, for $\alpha = 6{\cdot}9$ and a gap width of 6·4 mm; clearly the distribution is fairly symmetrical about the midplane and there is general agreement with the form of the theoretical curve derived from the first term in Equation 1 (see also Fig. 2) but the latter gives only a slight indication of the quite strong reverse flow seen at $\bar{z}/a \cong 0{\cdot}5$. The magnitude of the reverse flow depends on $r/r_o$, decreasing towards exit, and can be understood in terms of an entry effect, since $r/r_o = 0{\cdot}91$ only represents an entry length of about 20 gap widths. With the smaller gap (3·5 mm) there was less indication of reverse flow, but it was harder to make spatially resolved measurements. As $\alpha$

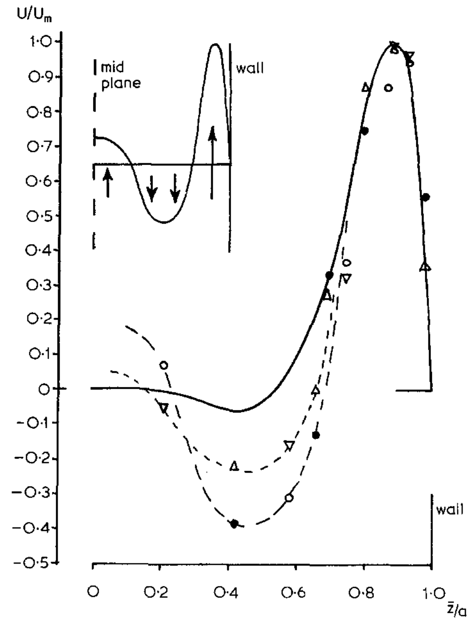


Fig. 5. Radial velocity distribution for $r/r_o$ values of 0·91 (▽ top semi-gap, △ bottom semi-gap) and 0·80 (○ top semi-gap, ● bottom semi-gap).

increases, the velocity in the reverse direction becomes relatively smaller, i.e. it is superimposed on a stronger outward flow. The absolute values of velocity at large $r/r_o$ agree with theoretical values [11] appropriate for a flow rate of about 1200 ml min$^{-1}$. The flow rate was not measured in these experiments but this value is reasonable in the light of later work [7]. At small values of $\alpha$ ($\lesssim 4$) a negative velocity was seen in the mid-

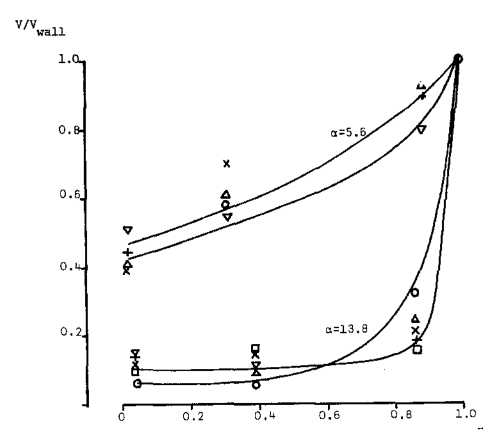


Fig. 6. Tangential velocity distribution for $r/r_o$ values of 0·27 (○), 0·42 (X), 0·57 (△), 0·72 (+), 0·88 (▽), 1·00 (□).

plane at all values of $r/r_0$, indicating that fluid was being ingested into the gap from the tank; had a source flow been applied at the centre rather than the cell being made to pump itself probably this would not have been the case. Studies are continuing with applied source flows [7].

Fig. 6 shows normalized tangential velocities for two values of $\alpha$. It is evident that the fluid as a whole rotates and that at low $\alpha$ this approaches a solid body rotation. However, as $\alpha$ increases the tangential shear stress increases to such an extent that the velocity gradient becomes increasingly localized at the wall. Although there is some scatter on the data (due mainly to errors of location) note also that the velocity gradient increases with increasing $r/r_0$.

## 5. Discussion

The laser–Doppler measurements show that the double-humped radial velocity distribution predicted by Kreith can be realized in practice even when the system is self-pumping so that the source flow is self-induced. Further, Fig. 5 and other data show that the spacing pillars do not seriously affect the flow so that an electrolyser can be built in which low-speed rotation of the whole assembly occurs. Similarly, Fig. 6 and other data show that swirl is induced in the electrolyte, but that for Taylor numbers of order 10 most of the electrolyte rotates at less than 20% of the wall velocity. These results suggest that it will be possible to separate anolyte and catholyte streams permanently at exit from the cell by using an annular splitter plate in the midplane [4] without grossly perturbing the flow. Such studies are continuing at present.

As $\alpha$ increases, the radial velocity maximum approaches the wall more closely (for example, see Figs. 2 and 3) and the velocity gradient at the wall increases, however the tangential velocity gradient also increases and it is not clear, *ab initio*, whether the radial or tangential velocity controls mass transport at the wall. Further, the coupling of radial and tangential velocities suggest recirculation and implies that the cross-gap transport of reactive species may be so high that the separation of streams is negated in electrosynthesis; this depends on the dispersion of species generated at the wall. The questions of mass transport to the electrode and dispersion from the electrode are dealt with in Part II.

## References

[1] R. Dworak and H. Wendt, *Ber. Bunsengesellschaft Phys. Chem.* **80** (1976) 78.
[2] M. Fleischmann, R. E. W. Jansson and R. J. Marshall (to be published).
[3] M. Fleischmann, R. E. W. Jansson and J. Ghoroghchian (to be published).
[4] M. Fleischmann, R. E. W. Jansson and R. J. Marshall, Brit. Prov. Pat. 04939/76 (April 1976).
[5] F. Kreith, *Internat. J. Heat Mass Transfer* 9 (1966) 265.
[6] H. G. Thomas and E. Lux, *Tetrahedron Letters* **10** (1972) 965.
[7] A. Ferreira, R. E. W. Jansson and R. J. Marshall (to be published).
[8] O. F. Ferreira, Ph.D. Thesis, University of Southampton (1978).
[9] O. F. Ferreira, R. E. W. Jansson and J. E. Rizzo, 'Correlation of Mass Transfer and Laser–Doppler Information', Proceedings of LDA Symposium, Lynby, Denmark (1975).
[10] O. F. Ferreira and R. E. W. Jansson, 'Local Measurements in Parallel Plate Cells', 27th Meeting ISE, Zürich, Switzerland (1976).
[11] R. E. W. Jansson 'Flow field in the rotating electrolyser' (to be published).